

Air Gaps as Intermediate Selective Reflectors to Reach Theoretical Efficiency Limits of Multibandgap Solar Cells

Vidya Ganapati, Chi-Sing Ho, and Eli Yablonovitch

Abstract—Efficient external luminescence is a prerequisite for high-voltage solar cells. To approach the Shockley–Queisser limit, a highly reflective rear mirror is required. This mirror enhances the voltage of the solar cell by providing internally luminescent photons with multiple opportunities for escaping out the front surface. Likewise, intermediate reflectors in a multibandgap solar cell can assist external luminescence to enhance the voltage for each cell in a stack. These intermediate reflectors must also transmit the subbandgap photons to the next cell in the stack. A practical implementation of an intermediate selective reflector is an air gap sandwiched by antireflection coatings. The air gap provides perfect reflection for angles outside the escape cone, and the antireflection coating transmits angles inside the escape cone. As the incoming sunlight is within the escape cone, it is transmitted on to the next cell, while most of the internally trapped luminescence is reflected. We calculate that air gap intermediate reflectors, along with a rear mirror, can provide an absolute efficiency increase of $\approx 5\%$ in multibandgap cells.

Index Terms—Detailed balance limit, intermediate reflector, mirror, multijunction solar cell, quasi-equilibrium.

I. INTRODUCTION

OVER the past few years, the efficiency record for a single-bandgap 1-sun solar cell has risen to 28.8% [1]: a record held by a thin-film gallium arsenide cell from Alta Devices. This efficiency increase was enabled by improving the efficiency of luminescence extraction from the solar cell [2], [3]. This record-holding single-bandgap cell had a rear reflector, rather than a substrate. In a solar cell, some of the absorbed photons will radiatively be emitted as luminescence. These internally luminescent photons can then be reabsorbed in the cell or escape from a surface. In an ideal solar cell with a perfect rear mirror, at open circuit, all the absorbed photons will be re-emitted and will eventually escape from the top surface. A good rear reflector provides multiple opportunities for a luminescent photon to escape out of the front surface of the cell and was

Manuscript received June 10, 2014; revised August 11, 2014 and September 15, 2014; accepted September 24, 2014. Date of publication October 15, 2014; date of current version December 18, 2014. The work of V. Ganapati was supported as part of the U.S. Department of Energy (DOE) “Light-Material Interactions in Energy Conversion” Energy Frontier Research Center under Grant DE-SC0001293. The work of C.-S. Ho was supported by the U.S. DOE under Contract DE-AC36-08-GO28308 with the National Renewable Energy Laboratory.

The authors are with the University of California, Berkeley, Berkeley, CA 94720 USA (e-mail: vidyag@berkeley.edu; csho@stanford.edu; eliy@eecs.berkeley.edu).

Color versions of one or more of the figures in this paper are available online at <http://ieeexplore.ieee.org>.

Digital Object Identifier 10.1109/JPHOTOV.2014.2361013

instrumental in achieving the single-bandgap solar cell record efficiency [2].

In a multijunction solar cell, bandgaps of different materials are placed in a stack, from the largest bandgap on top to the smallest on the bottom. The top cell absorbs all the photons above its bandgap, and the lower energy photons are transmitted to the next bandgap. In the past year, a new record of 31.1% was set by the National Renewable Energy Laboratory, for a dual-bandgap solar cell under 1-sun illumination, by using a rear reflector to improve the voltage in the bottom cell [4]. In a multijunction solar cell stack, improving the rear reflector improves the voltage of the bottommost cell; however, the upper cells do not get this same voltage boost. In order to further improve the efficiency of a dual-bandgap solar cell, an intermediate reflector needs to be placed in between the top and bottom cells. This intermediate reflector needs to reflect the internally luminescent photons (which are mostly at the bandgap energy, arriving at all angles), but transmit the subbandgap photons to the next cell below. These subbandgap photons are near normal incidence, owing to the refraction from air into the higher index solar cell material.

II. THEORY

The quasi-equilibrium derivation given by Shockley and Queisser [5] yields the limiting efficiency of a solar cell with one material bandgap. In [6]–[11], the analysis to multiple bandgaps is extended, obtaining the limiting efficiencies with multiple material bandgaps. Of these, in [6], [7], and [10], the case where the subcells are electrically connected in series is analyzed; therefore, each subcell must operate at the same current. In our following theoretical analysis of the multibandgap cell, we assume that each subcell is electrically independent (i.e., each subcell has two terminal connections), in order to find limiting efficiencies. In [8], [10], and [11], the case is examined where there are no intermediate reflectors, and all the subcells are index matched. Multijunction cells with intermediate reflectors were analyzed in [6] and [8], but the effect of improved luminescence extraction in boosting the voltage was not accounted for. Here, we account for the voltage boost that arises from improved external luminescent extraction from each bandgap of a tandem cell.

We derive the limiting efficiency of multibandgap cells following a similar procedure to the derivation for single-bandgap cells in [2]. We assume step function absorption (all photons above the bandgap energy are absorbed, and all photons below the bandgap energy are transmitted).

We will first consider the top cell, which consists of the material with the largest bandgap, E_{g1} . The analysis of this top cell is identical to the single-bandgap case derived in [2]. The analysis begins in the dark, at thermal equilibrium, with the cell absorbing blackbody radiation from the external environment. The blackbody radiation $b(E)$ can be approximated by the tail of the blackbody formula:

$$b(E) = \frac{2E^2}{h^3 c^2} \exp\left(-\frac{E}{kT}\right) \quad (1)$$

where the units of b are [photons/(time \times area \times energy \times steradian)], E is the photon energy, h is Planck's constant, c is the speed of light, and kT is the thermal energy.

The photon flux through the front surface of the solar cell due to absorption of the blackbody is given as

$$L_{bb} = 2\pi \int_0^\infty \int_0^{\frac{\pi}{2}} a(E) b(E) \sin \theta \cos \theta d\theta dE \quad (2)$$

where θ is the angle from the normal to the cell, and $a(E)$ is the step function absorptivity for E_{g1} . The 2π factor arises from the integration over the azimuthal angle φ . Since the cell is in thermal equilibrium, L_{bb} is also equivalent to the photon flux emitted out of the front surface.

When the sun illuminates the cell, it moves into quasi-equilibrium, with chemical potential qV (this is equivalent to the separation of the quasi-Fermi levels, where q is the charge of an electron and V is the voltage). Under illumination, the photon flux out the front of the cell, i.e., L_{ext} , is given by

$$\begin{aligned} L_{ext}(V) &= e^{\frac{qV}{kT}} \times L_{bb} \\ &= e^{\frac{qV}{kT}} \times 2\pi \int_{E_{g1}}^\infty \int_0^{\frac{\pi}{2}} b(E) \sin \theta \cos \theta d\theta dE \end{aligned} \quad (3)$$

where we have represented the step function absorptivity $a(E)$ through the limits of integration.

The external luminescence yield, η_{ext} , is defined as the ratio of the rate of radiative flux out the top, L_{ext} , to the total loss rate of photons from the cell. We assume the cell is free of nonradiative recombination in this analysis. Thus, the total loss rate of photons is given as $L_{ext} + L_{int\downarrow}$, where $L_{int\downarrow}$ is the radiative flux out the bottom to the next cell below:

$$\eta_{ext} = \frac{L_{ext}}{L_{ext} + L_{int\downarrow}}. \quad (4)$$

The current of the solar cell is given by the absorption of photons from the sun minus the emission of photons out of the cell. The absorption of photons from the sun is $\int a(E) S(E) dE$, where S is the number of photons in the solar spectrum per unit area per unit time. From (4), we obtain $L_{ext} + L_{int\downarrow} = \frac{L_{ext}}{\eta_{ext}}$. Thus, the $J-V$ characteristic of the top cell in the tandem stack is given by

$$\begin{aligned} J_1(V_1) &= \int_{E_{g1}}^\infty S(E) dE - L_{ext} - L_{int\downarrow} \\ &= \int_{E_{g1}}^\infty S(E) dE - \frac{1}{\eta_{ext}} \pi e^{\frac{qV_1}{kT}} \int_{E_{g1}}^\infty b(E) dE \end{aligned} \quad (5)$$

where J_1 is the current density, and V_1 is the voltage of the top cell. Equation (5) makes the approximation $e^{\frac{qV_1}{kT}} - 1 \approx e^{\frac{qV_1}{kT}}$. To extract the maximum power from the top cell, the value of V_1 should be chosen to be the maximum power point of the cell.

The expression for the open-circuit voltage of the top cell is given by setting $J_1 = 0$ in (5):

$$V_{oc,1} = \frac{kT}{q} \ln \left(\frac{\int_{E_{g1}}^\infty S(E) dE}{\pi \int_{E_{g1}}^\infty b(E) dE} \right) - \frac{kT}{q} \ln \left(\frac{1}{\eta_{ext}} \right). \quad (6)$$

From (6), we see that the open-circuit voltage penalty from ideal when $\eta_{ext} < 1$ is $\frac{kT}{q} \ln(\frac{1}{\eta_{ext}})$.

We now consider the second cell beneath the first cell. The absorption of photons from the sun is now given as $\int_{E_{g2}}^{E_{g1}} S(E) dE$ (assuming step function absorptivity for the second cell as well). In the $J-V$ characteristic of the second cell, there is an extra term to account for the radiative flux out of the bottom of the top cell that is absorbed by the second cell. Since from (4), $L_{int\downarrow} = \frac{L_{ext}}{\eta_{ext}} - L_{ext}$, the downward flux is given by

$$L_{int\downarrow} = \left(\frac{1}{\eta_{ext}} - 1 \right) \pi e^{\frac{qV_1}{kT}} \int_{E_{g1}}^\infty b(E) dE. \quad (7)$$

By analogy to (5), the $J-V$ characteristic of the second cell is, thus, given by

$$\begin{aligned} J_2(V_2, V_1) &= \int_{E_{g2}}^{E_{g1}} S(E) dE + \left(\frac{1}{\eta_{ext,1}} - 1 \right) \pi e^{\frac{qV_1}{kT}} \\ &\quad \int_{E_{g1}}^\infty b(E) dE - \frac{1}{\eta_{ext,2}} \pi e^{\frac{qV_2}{kT}} \int_{E_{g2}}^\infty b(E) dE \end{aligned} \quad (8)$$

where $\eta_{ext,1}$ refers to the external fluorescence yield of the top cell, and $\eta_{ext,2}$ refers to the second cell. The derivation of the $J-V$ characteristic for cells below the second follows the same procedure as the second cell.

In order to obtain the efficiency of a multibandgap device, the optimal power point, i.e., $V_{1,max}$, is first determined for the topmost cell, and the power extracted is calculated by $P_{1,max} = V_{1,max} \times J_1(V_{1,max})$. The optimal power point $V_{2,max}$ is then found by maximizing $P(V_2, V_1 = V_{1,max}) = V_2 \times J_2(V_2, V_1 = V_{1,max})$. To find the efficiency, the power extracted from each subcell is summed and is divided by the total incident power from the sun impinging on the area of the cell.

III. STRUCTURES

We consider several versions of multibandgap solar cells with different intermediate reflectors. We consider the cases of 1) no intermediate reflector and no rear mirror, 2) no intermediate reflector and a perfect rear mirror, and 3) an air gap as the intermediate layer and a perfect rear mirror.

A. Case 1: No Intermediate Reflector, No Rear Mirror

We first consider the case of a dual-bandgap solar cell without an intermediate reflector or rear mirror [see Fig. 1(a)]. The top and bottom cells are index matched, on an absorbing substrate, and we assume a perfect antireflection coating on the top cell. We consider the following two cases, i.e., cases (1a) and (1b), where

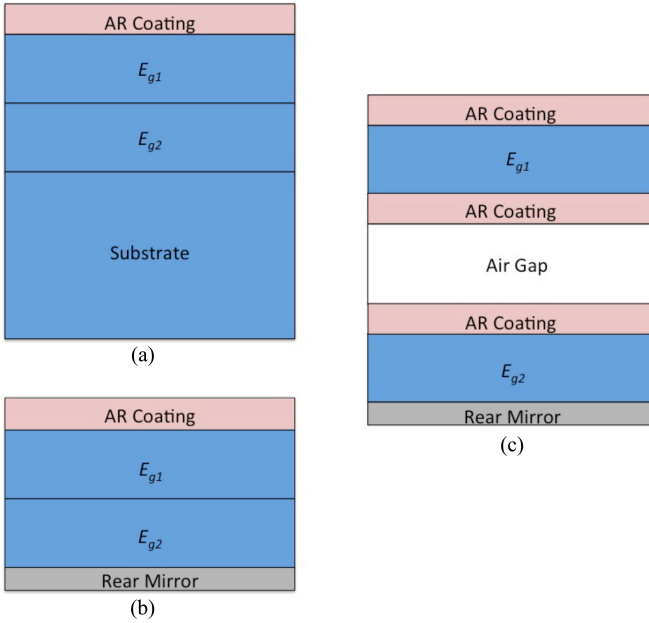


Fig. 1. (a) Case 1a. A multibandgap solar cell without an intermediate or a rear mirror; the top cell, bottom cell, and substrate are index matched with $n_s = 3.5$. In case 1a, the subcells are optically thin to the luminescent photons; in case 1b, the cells are optically thick. (b) Case 2. No intermediate reflector, with a perfect rear mirror. In case 2a, the top cell is assumed to be optically thin to the internal luminescence, and in case 2b, the top cell is optically thick. (c) Case 3. The subcells are separated by an air gap intermediate reflector, with perfect antireflection (AR) coatings and a perfect rear mirror.

the cells are optically thin and optically thick to the internal luminescence, respectively. Perfect antireflection coatings and zero nonradiative recombination are assumed throughout.

1) Case 1a: No Intermediate Reflector, No Rear Mirror, Optically Thin Cells: In Case 1a, we assume that the cells are optically thin to the luminescent photon energies. This assumption means that the cell is weakly absorbing near the luminescent energies (the energies at which absorbed photons are re-emitted as), although it can still be strongly absorbing at higher energies (hence, the assumption of step function absorption is still valid).

The external luminescence yield η_{ext} can also be described as the probability that an absorbed photon escapes out the front surface [2]. For the limit of a very optically thin cell, we can determine that $\eta_{\text{ext}} \approx \frac{1}{4n_s^2}$ by recognizing that the probability of front surface escape, relative to substrate absorption, is the fraction of solid angle that is subtended by the escape cone [12]. We can derive η_{ext} for case 1a as follows:

$$\eta_{\text{ext}} = \frac{2\pi \int_0^{\sin^{-1}(\frac{1}{n_s})} \sin \theta d\theta}{2\pi \int_0^\pi \sin \theta d\theta} \approx \frac{1}{4n_s^2}. \quad (9)$$

2) Case 1b: No Intermediate Reflector, No Rear Mirror, Optically Thick Cells: In Case 1b, we assume that the cells are optically thick. We assume that the solar cell is in air with index of refraction $n = 1$, with a perfect antireflection coating on the top. Thus, at the top surface, we can assume perfect transmittance of internally luminescent photons in the escape cone θ_s (given by Snell's law, $n_s \sin \theta_s = 1$, where n_s is the refractive

index of the top semiconductor). There is total internal reflection for internal luminescent photons outside the escape cone. We assume that the internal luminescence hitting the top surface has a Lambertian distribution, as is typical of optically thick material. The angle-averaged transmittance of the internally luminescent photons through the top surface, $T_{\text{int}\uparrow}$, is thus given by

$$T_{\text{int}\uparrow} = \frac{2\pi \int_0^{\sin^{-1}(\frac{1}{n_s})} \sin \theta \cos \theta d\theta}{2\pi \int_0^{\frac{\pi}{2}} \sin \theta \cos \theta d\theta} = \frac{1}{n_s^2}. \quad (10)$$

Since the cell is free of nonradiative recombination, the only other photon flux out of the cell is out the rear surface, which is described by rear luminescent transmittance $T_{\text{int}\downarrow}$. $T_{\text{int}\downarrow}$ is unity because the top and bottom cell are assumed to be index matched with no intermediate layer between them. Applying (4) and (10) yields

$$\eta_{\text{ext}} = \frac{T_{\text{int}\uparrow}}{T_{\text{int}\uparrow} + T_{\text{int}\downarrow}} = \frac{1}{1 + n_s^2}. \quad (11)$$

We have a factor of $\approx \frac{1}{4}$ difference in η_{ext} between the cases of optically thin and thick. The impact of absorption on η_{ext} is discussed further in [13].

B. Case 2: No Intermediate Reflector, Perfect Rear Mirror

The second case we consider is a multibandgap solar cell without an intermediate reflector, with a perfect rear mirror [see Fig. 1(b)]. The top and bottom cells are index matched, and we assume a perfect antireflection coating on the top cell. We again consider two cases, i.e., cases 2a and 2b, where the cells are optically thin and optically thick to the internal luminescence, respectively.

1) Case 2a: No Intermediate Reflector, Perfect Rear Mirror, Optically Thin Cells: We have $\eta_{\text{ext},2} = 1$ for the bottom cell (due to the perfect rear mirror), and $\eta_{\text{ext},1} = \frac{1}{4n_s^2}$ for the top cell, as in case 1a.

2) Case 2b: No Intermediate Reflector, Perfect Rear Mirror, Optically Thick Cell: We have $\eta_{\text{ext},2} = 1$ for the bottom cell (due to the perfect rear mirror), and $\eta_{\text{ext},1} = \frac{1}{1+n_s^2}$ for the top cell, as in case 1b.

C. Case 3: Air Gap Intermediate Reflector, Perfect Rear Mirror

The final case we consider is a multibandgap solar cell with an intermediate reflector between the cells and a perfect rear mirror. An intermediate reflector for a multibandgap cell must satisfy the requirements of 1) reflecting the internally luminescent photons of the top cell and 2) transmitting the externally incident photons that are below the bandgap of the top cell.

These dual requirements for an intermediate reflector appear difficult to satisfy. However, air gaps provide the following advantages:

- 1) We obtain total internal reflection for the photons outside of the escape cone. In this paper, we assume $n_s = 3.5$ for the refractive indices of all the cells. Due to the large refractive index mismatch with air ($n = 1$), the escape cone given by Snell's law is $\sin^{-1}(\frac{1}{3.5}) \approx 17^\circ$ from the

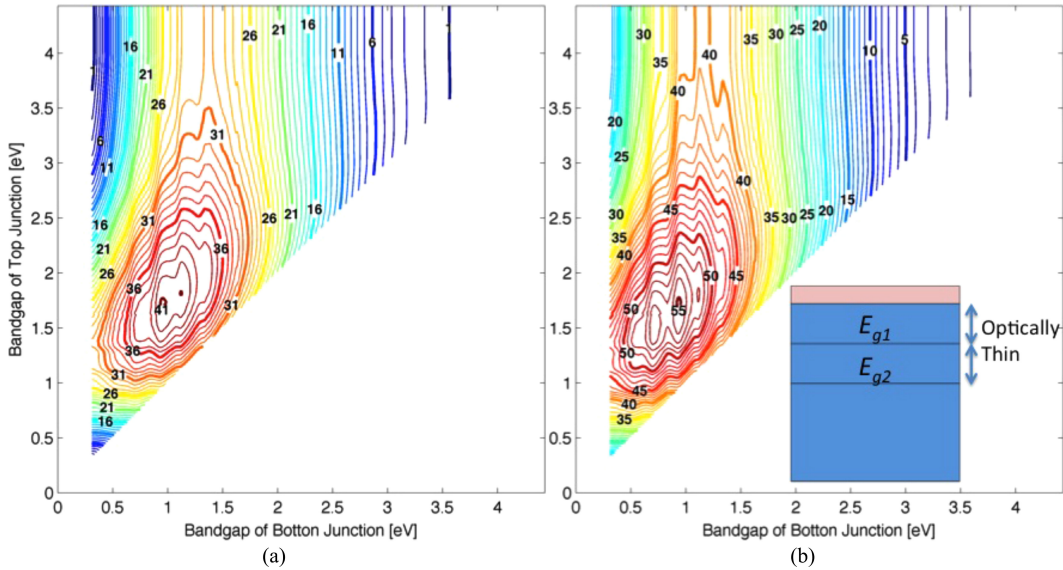


Fig. 2. Efficiencies as a function of top and bottom bandgap for case 1a, a dual-junction solar cell without an intermediate or a rear mirror; the cells are assumed to be optically thin to the internally luminescent photons. (a) Efficiencies under 1 sun and (b) the efficiencies under 46 211-sun concentration.

normal. Most of the internally luminescent photons are thus outside the escape cone and are reflected.

- 2) The externally incident photons, upon entrance into our structure, refract into the escape cone of the top cell material, as described by Snell's law. Thus, we can use anti-reflection coatings to transmit the photons in the escape cone to the next cell.

The internally luminescent photons are created at all angles, while the transmitted solar photons have a limited angular range. Thus angular filtering by the air gap can be used to obtain spectral filtering, in order to recycle the luminescent photons. For case 3, we assume an air gap for the intermediate reflector, sandwiched by perfect antireflection coatings, as well as a perfect rear mirror and perfect top antireflection coating [see Fig. 1(c)]. In this scenario, $\eta_{\text{ext},1} = 0.5$, since there is equal luminescent extraction from the front and back interfaces of the top cell. With a perfect back mirror, $\eta_{\text{ext},2} = 1$, since all the photons must eventually escape out the front of the device. In case 3, we obtain the same η_{ext} whether the cells are optically thick or optically thin to the internal luminescence.

IV. RESULTS AND DISCUSSION

The efficiencies for cases 1–3 are computed as a function of top and bottom bandgaps. In our calculations, we assume cell temperature of $T = 30^\circ\text{C}$, two terminal connections to each subcell, and an index of refraction of $n_s = 3.5$ (a typical semiconductor refractive index) for all the subcells. The radiation from the sun is modeled with the Air Mass 1.5 Global tilt spectrum [14]. We plot the efficiencies both under 1 sun and also under the maximum concentration achievable, 46 211 suns (in the case of concentration, $S(E) = 46211 \times S_{\text{AM}1.5}(E)$, where $S_{\text{AM}1.5}(E)$ is the Air Mass 1.5 Global tilt spectrum).

TABLE I
EFFICIENCIES FOR THE OPTIMAL DUAL-BANDGAP CELL FOR CASES 1-3

	E_{g1} [eV]	E_{g2} [eV]	Efficiency
Case 1a: 1 Sun	1.73	0.95	41.1%
Case 1a: 46 211 Suns	1.73	0.93	55.2%
Case 1b: 1 Sun	1.73	0.95	42.8%
Case 1b: 46 211 Suns	1.73	0.93	56.9%
Case 2a: 1 Sun	1.81	0.95	44.0%
Case 2a: 46 211 Suns	1.74	0.93	58.2%
Case 2b: 1 Sun	1.73	0.94	44.7%
Case 2b: 46 211 Suns	1.73	0.93	58.9%
Case 3: 1 Sun	1.73	0.94	45.7%
Case 3: 46 211 Suns	1.53	0.70	60.0%

In Figs. 2–6, we plot the efficiencies as a function of top and bottom bandgap for cases 1a, 1b, 2a, 2b, and 3, respectively. The efficiencies are plotted both under 1 sun and 46 211 suns. Our range of bandgap energies corresponds to the range of energies in the Air Mass 1.5 Global tilt spectrum. The main feature of these contour plots is a double peak around the optimal bandgaps. There is also a region of vertical lines, where adding a top subcell to a bottom subcell does not significantly increase the efficiency of the tandem cell. This region occurs because the top subcell has too large of a bandgap and consequently does not absorb many photons.

We extract the optimal bandgaps from each of these plots and list them in Table I. The absolute difference between the limiting efficiency in case 1a and 3 is 4.6%. Thus, in the case where the cell is optically thin to the internal luminescence, an absolute efficiency increase of 4.6% is available with proper intermediate and rear mirror design. Although the air gap presents manufacturing difficulties, it is a feasible architecture, as demonstrated experimentally in [17].

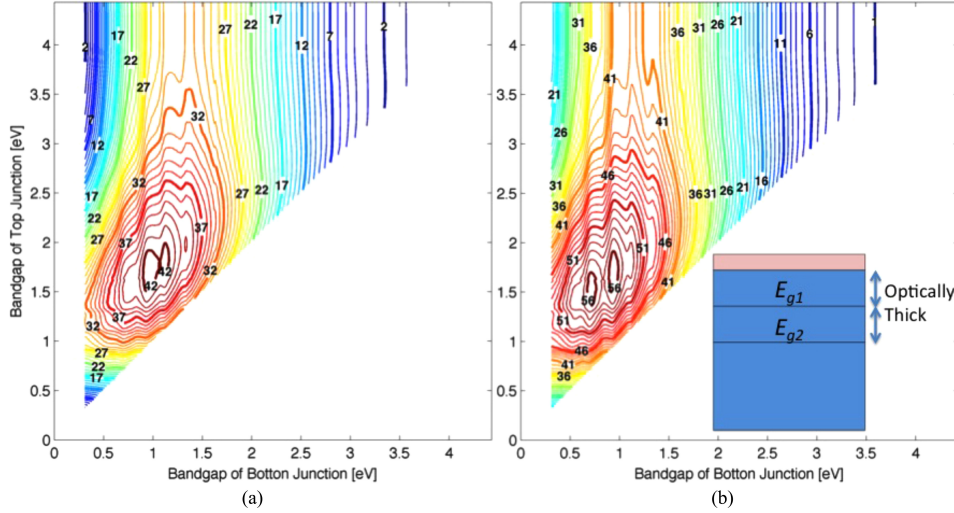


Fig. 3. Efficiencies as a function of top and bottom bandgap for case 1b, which is a dual-junction solar cell without an intermediate or a rear mirror; the cells are assumed to be optically thick to the internally luminescent photons. (a) Efficiencies under 1 sun and (b) the efficiencies under 46 211-sun concentration.

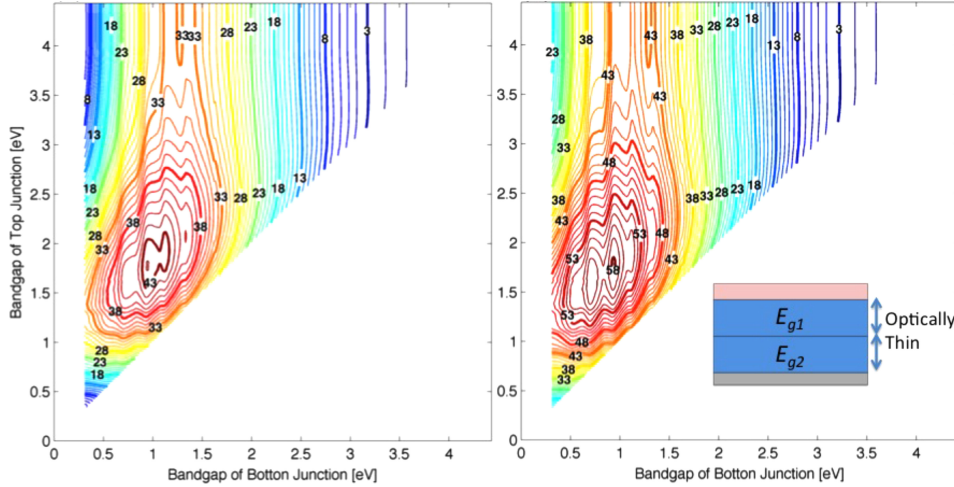


Fig. 4. Efficiencies as a function of top and bottom bandgap for case 2a, which is a dual-junction solar cell without an intermediate reflector, with a perfect rear mirror; the cells are assumed to be optically thin to the internally luminescent photons. (a) Efficiencies under 1 sun and (b) the efficiencies under 46 211-sun concentration.

In [4], [15], and [16], the authors achieve experimental efficiencies of 31.1%, 30.8%, and 30.3%, respectively, for the tandem cell of InGaP ($E_g = 1.8$ eV) on GaAs ($E_g = 1.4$ eV). We extract the limiting efficiencies from Figs. 2–6 for these materials and list in Table II. For this combination of bandgaps, the absolute efficiency increase from cases 1a to 3 under 1 sun is 2.7%.

To isolate the effect of the air gap intermediate reflector, we look at case 2a, a dual-bandgap solar cell with no intermediate reflector and a perfect rear mirror; see Fig. 1(b). The top cell is assumed to be optically thin to the internal luminescence. In Fig. 7, we plot the open-circuit voltage of the top cell, short-circuit current of the bottom cell, and overall cell efficiency for cases 2a and 3, the case with the air gap intermediate reflector and perfect rear mirror. The optimal bandgaps from case 3, the ideal case, are used in this calculation ($E_{g1} = 1.73$ eV and $E_{g2} = 0.94$ eV). The optimal bandgaps for case 2a are within

TABLE II
EFFICIENCIES FOR A DUAL-BANDGAP CELL, $E_{g1} = 1.8$ AND $E_{g2} = 1.4$

	1-Sun Concentration	46 211-Sun Concentration
Case 1a No intermediate reflector, no rear mirror, optically thin	37.3%	46.4%
Case 1b No intermediate reflector, no rear mirror, optically thick	38.4%	47.4%
Case 2a No intermediate reflector, perfect rear mirror, optically thin	38.6%	47.7%
Case 2b No intermediate reflector, perfect rear mirror, optically thick	39.3%	48.3%
Case 3 Air gap intermediate reflector, perfect rear mirror	40.0%	49.1%

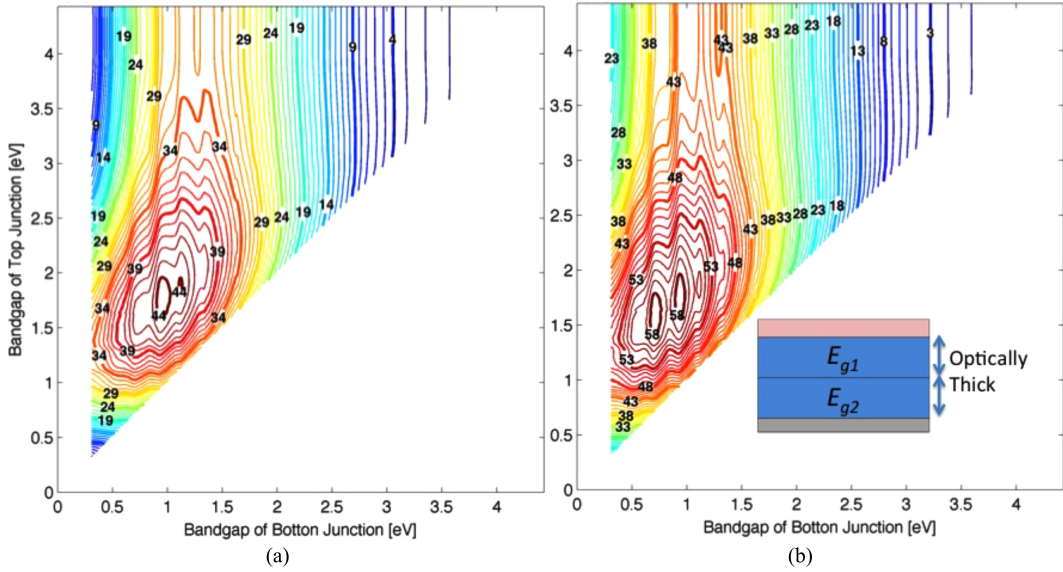


Fig. 5. Efficiencies as a function of top and bottom bandgap for case 2b, which is a dual-junction solar cell without an intermediate reflector, with a perfect rear mirror; the cells are assumed to be optically thick to the internally luminescent photons. (a) Efficiencies under 1 sun and (b) the efficiencies under 46 211-sun concentration.

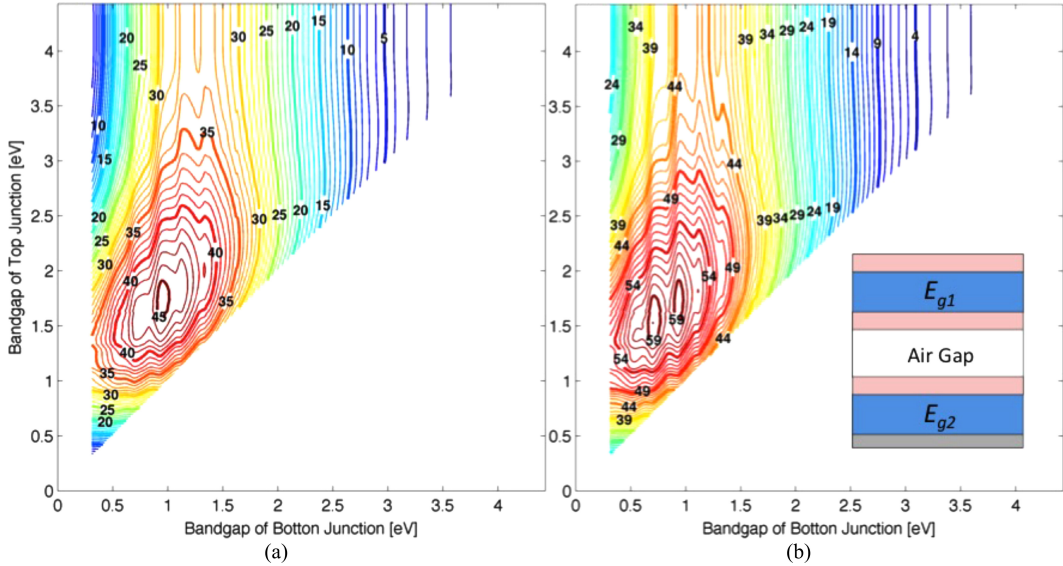


Fig. 6. Efficiencies as a function of top and bottom bandgap for case (3), which is a dual-junction cell with an air gap intermediate reflector and perfect rear mirror. (a) Efficiencies under 1 sun and (b) the efficiencies under 46 211-sun concentration.

0.1 eV of these bandgaps; therefore, this is a fair comparison.

Equation (6) allows us to calculate the open-circuit voltage penalties from the ideal case of a rear reflector that perfectly reflects all internal luminescence. The thermal voltage is 26 mV therefore, in case 3, with the air gap intermediate reflector, the top cell sees a voltage drop of $26 \text{ mV} \times \ln 2 = 18 \text{ mV}$ from ideal. With no intermediate reflector, and an optically thin top cell as in case 2a, the top cell sees a voltage drop of $26 \text{ mV} \times \ln \{4n_s^2\} = 100 \text{ mV}$ from ideal, with $n_s = 3.5$. Thus, as we see in Fig. 7, the top cell voltage difference between cases 3 and 2a is $\approx 80 \text{ mV}$.

As a result of the intermediate reflector, there is also a slight decrease in current in the bottom cell. This current decrease is due to the loss of radiative emission out the rear of the top cell that is then absorbed by the bottom cell. The effect of current loss in the bottom cell is minor compared with the gain in voltage of the top cell with the intermediate reflector. Thus, for case 3 minus case 2a, we see a tandem efficiency increase of 1.7%, solely due to the air gap intermediate reflector.

Using the same methodology, we calculate the limiting efficiency of multibandgap cells with one through six bandgaps, for cases (1a), (1b), (2a), (2b), and (3); see Table III. The efficiencies

TABLE III
EFFICIENCIES FOR CELLS WITH ONE THROUGH SIX BANDGAPS, FOR CASES 1–3, UNDER 1 SUN

E_{g1} [eV]	E_{g2} [eV]	E_{g3} [eV]	E_{g4} [eV]	E_{g5} [eV]	E_{g6} [eV]	Case 1a No intermediate reflectors, no rear mirror, optically thin	Case 1b No intermediate reflectors, no rear mirror, optically thick	Case 2a No intermediate reflectors, perfect rear mirror, optically thin	Case 2b No intermediate reflectors, perfect rear mirror, optically thick	Case 3 Air gap intermediate reflectors, perfect rear mirror
1.34						30.1%	31.3%	—	—	—
1.73	0.94					41.1%	42.8%	44.0%	44.7%	45.7%
2.04	1.40	0.93				47.1%	48.8%	49.0%	50.1%	51.5%
2.23	1.63	1.14	0.702			50.4%	52.3%	52.1%	53.5%	55.3%
2.39	1.83	1.37	0.97	0.695		52.9%	54.9%	54.1%	55.7%	57.7%
2.53	2.02	1.64	1.34	0.96	0.694	54.7%	56.7%	55.8%	57.4%	59.4%

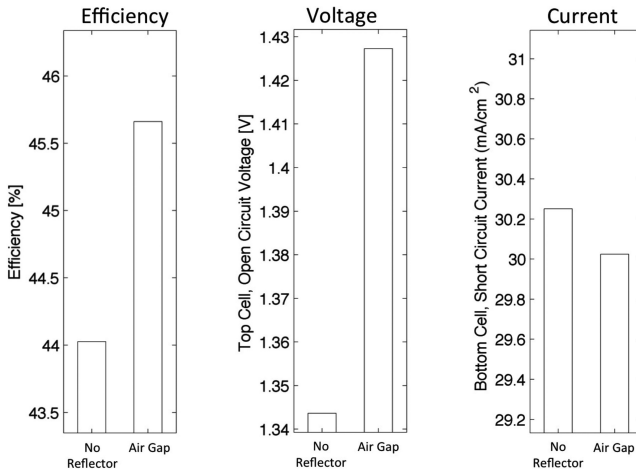


Fig. 7. Tandem cell efficiency, top cell open-circuit voltage, and bottom cell current for bandgaps $E_{g1} = 1.73$ eV and $E_{g2} = 0.94$ eV, for case 2a, with no intermediate reflector and with a perfect rear mirror, assuming cells that are optically thin to the internal luminescence, and case 3, which has an air gap intermediate reflector and a perfect rear mirror.

for the one to three cell stacks are calculated at the optimal bandgaps for case 3. The bandgaps for four to six cells are taken from [6], as the optimization of four or more bandgap cells is out of the scope of this paper (the bandgaps taken from [6] are for the case of electrically independent subcells).

We see an increase of $\approx 1\%$ absolute by adding an intermediate reflector for cells that are optically thick to the luminescence, case 3 minus case 2b, for the dual-bandgap cell. In the work by Martí and Araújo [8], the efficiency boost calculated from adding an intermediate reflector in a similar situation is only $\approx 0.2\%$ absolute. This is because there is no refractive index mismatch with air in their work. Consequently, an intermediate reflector to assist in the recycling of photons in the top cell in their calculations has minimal effect on the open-circuit voltage, as the photons already have a significantly higher probability of escape.

When we make the comparison with the optically thin case rather than the optically thick case, we see a greater boost in efficiency with proper mirror design. In a real material, the absorption of the luminescence depends on the degree of overlap between the luminescence spectrum and absorption spectrum. As absorption is usually low near the band-edge, the assumption

of being optically thin to the internal luminescence can be a reasonable approximation. However, for real materials, η_{ext} will fall between the limiting values we derive for optically thin and thick.

V. CONCLUSION

An intermediate reflector has the dual burden of reflecting the internally luminescent photons and transmitting below bandgap photons. We, thus, propose an air gap sandwiched with antireflection coatings to serve as the intermediate reflector, using angular selectivity by total internal reflection to achieve frequency selectivity. Together with a perfect rear mirror, this results in an $\approx 5\%$ absolute efficiency improvement over cells without mirrors.

Future work can take into account the detailed absorption spectrum of real materials, nonradiative recombination, the actual quality of the antireflection coatings, shading losses between cells, resistive losses from introducing contact fingers above and below each cell, and the actual differing indices of refraction for the subcells, among other nonidealities.

ACKNOWLEDGMENT

The authors would like to acknowledge Dr. M. Steiner for helpful discussions regarding the difference between the optically thin and thick cases.

REFERENCES

- [1] M. A. Green, K. Emery, Y. Hishikawa, W. Warta, and E. D. Dunlop, "Solar cell efficiency tables (version 43): Solar cell efficiency tables," *Prog. Photovoltaic Res. Appl.*, vol. 22, no. 1, pp. 1–9, 2014.
- [2] O. D. Miller, E. Yablonovitch, and S. R. Kurtz, "Strong internal and external luminescence as solar cells approach the Shockley-Queisser limit," *IEEE J. Photovolt.*, vol. 2, no. 3, pp. 303–311, Jul. 2012.
- [3] O. D. Miller, "Photonic design: From fundamental solar cell physics to computational inverse design," Ph.D. dissertation, Dept. Elect. Eng. Comput. Sci., Univ. Calif., Berkeley, CA, USA, 2012.
- [4] (2012, Jun. 9). NREL Reports 31.1% Efficiency for III-V Solar Cell, [Online]. Available: <http://www.nrel.gov/news/press/2013/2226.html>
- [5] W. Shockley and H. J. Queisser, "Detailed balance limit of efficiency of p-n junction solar cells," *J. Appl. Phys.*, vol. 32, no. 3, pp. 510–519, 1961.
- [6] A. S. Brown and M. A. Green, "Detailed balance limit for the series constrained two terminal tandem solar cell," *Phys. E Low-Dimens. Syst. Nanostructures*, vol. 14, nos. 1/2, pp. 96–100, 2002.
- [7] C. H. Henry, "Limiting efficiencies of ideal single and multiple energy gap terrestrial solar cells," *J. Appl. Phys.*, vol. 51, no. 8, pp. 4494–4500, 2008.

- [8] A. Martí and G. L. Araújo, "Limiting efficiencies for photovoltaic energy conversion in multigap systems," *Sol. Energy Mater. Sol. Cells*, vol. 43, no. 2, pp. 203–222, 1996.
- [9] J. E. Parrott, "The limiting efficiency of an edge-illuminated multigap solar cell," *J. Phys. Appl. Phys.*, vol. 12, no. 3, pp. 441–450, 1979.
- [10] I. Tobías and A. Luque, "Ideal efficiency of monolithic, series-connected multijunction solar cells," *Prog. Photovoltaic Res. Appl.*, vol. 10, no. 5, pp. 323–329, 2002.
- [11] A. D. Vos, "Detailed balance limit of the efficiency of tandem solar cells," *J. Phys. Appl. Phys.*, vol. 13, no. 5, pp. 839–846, 1980.
- [12] E. Yablonovitch, "Statistical ray optics," *J. Opt. Soc. Amer.*, vol. 72, no. 7, pp. 899–907, 1982.
- [13] M. A. Steiner, J. F. Geisz, I. García, D. J. Friedman, A. Duda, and S. R. Kurtz, "Optical enhancement of the open-circuit voltage in high quality GaAs solar cells," *J. Appl. Phys.*, vol. 113, no. 12, pp. 123109-1–123109-10, 2013.
- [14] (2012, Jun. 9). Reference Solar Spectral Irradiance: Air Mass 1.5. [Online]. Available: rredc.nrel.gov/solar/spectra/am1.5
- [15] B. M. Kayes, L. Zhang, R. Twist, I. K. Ding, and G. S. Higashi, "Flexible thin-film tandem solar cells with >30% efficiency," *IEEE J. Photovoltaics*, vol. 4, no. 2, pp. 729–733, Mar. 2014.
- [16] T. Takamoto, E. Ikeda, H. Kurita, M. Ohmori, M. Yamaguchi, and M.-J. Yang, "Two-terminal monolithic In0.5Ga0.5P/GaAs tandem solar cells with a high conversion efficiency of over 30%," *Jpn. J. Appl. Phys.*, vol. 36, Part 1, no. 10, pp. 6215–6220, 1997.
- [17] X. Sheng, M. H. Yun, C. Zhang, A. M. Al-Okaily, M. Masouraki, L. Shen, S. Wang, W. L. Wilson, J. Y. Kim, P. Ferreira, X. Li, E. Yablonovitch, and J. A. Rogers, (2014). "Device architectures for enhanced photon recycling in thin-film multijunction solar cells," *Adv. Energy Mater.* [Online]. Available: <https://dx.doi.org/10.1002/aenm.201400919>

Authors' photographs and biographies not available at the time of publication.